ACS APPLIED MATERIALS & INTERFACES

RESEARCH ARTICLE

www.acsami.org

Graphene Supported Platinum Nanoparticle Counter-Electrode for Enhanced Performance of Dye-Sensitized Solar Cells

Reeti Bajpai,[†,‡] Soumyendu Roy,[†,‡] Pragyensh Kumar,[§] Preeti Bajpai,[§] Neha Kulshrestha,[†] Javad Rafiee,[⊥] Nikhil Koratkar,[⊥] and D. S. Misra*[,†]

[†]Department of Physics and [§]Department of Metallurgical Engineering and Materials Science, Indian Institute of Technology Bombay, Mumbai 400 076, India

[⊥]Department of Mechanical, Aerospace and Nuclear Engineering, Rensselaer Polytechnic Institute, 110 eighth Street, Troy, New York 12180, United States

ABSTRACT: Composites of few layered graphene (G) and platinum (Pt) nanoparticles (NP) with different loadings of Pt were used as counter electrode (CE) in dye-sensitized solar cell (DSSC). NPs were deposited directly on to G using pulsed laser ablation method (PLD). DSSCs formed using the composite CEs show improved performance compared to conventional Pt thin film electrode (Std Pt) and unsupported Pt NPs. Composite with 27% loading of Pt shows 45% higher efficiency (η = 2.9%), greater short circuit current (J_{sc} = 6.67 mA cm^{-2}), and open circuit voltage (V_{oc} = 0.74 V) without any loss of the fill factor (FF = 58%) as compared to the cells fabricated using Std Pt electrodes. Values of η, J_{sc} and V_{oc} for DSSC using Std Pt CE were 2%, 5.05 mA cm^{-2} and 0.68 V, respectively. Electrochemical impedance spectroscopy using I^-_3/I^- redox couple confirm lower values of charge transfer resistance for the composite electrodes, e.g., 2.36 Ω cm^2 as opposed to 7.73 Ω cm^2 of Std Pt. The better catalytic activity of these composite materials is also reflected in the stronger I^-_3 reduction peaks in cyclic voltammetry scans.

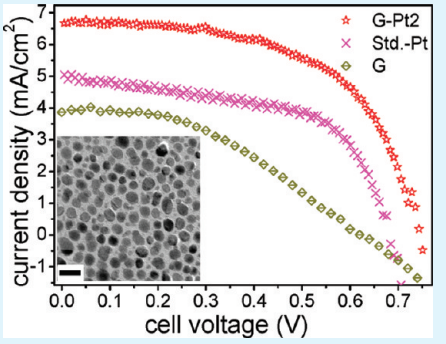

1. INTRODUCTION

Solid-state semiconductor devices have dominated the field of photovoltaics since its inception. Of late, dye-sensitized solar cell (DSSC) functioning at a molecular level has emerged as a viable alternative technology. Key attractions of this device include low cost, ease of fabrication, and better performance with diffused light. In addition, it provides unique design opportunities like flexibility, lightweight, transparency and color variation.[1−3] A typical DSSC consists of a photo active anode, an electrolyte with a redox couple, generally an iodide/triiodide (I^-/I^-_3) pair dissolved in an organic solvent, and a counter electrode (CE). The anode contains a thin layer of transparent conductive oxide (TCO) on a glass substrate. The TCO is coated with a mesoporous network of nanosized particles of a wide band gap semiconductor. The most commonly used semiconductor is titanium dioxide (TiO_2). A single molecule layer of dye (usually a ruthenium dye) is adsorbed onto the surface of TiO_2 particles. On exposure to light electrons in the dye molecule are excited from the HOMO to LUMO energy level. This electron is then injected into the conduction band of the semiconductor and transported by concentration gradient onto the TCO anode. The redox species present in the electrolyte work as mediators transferring electrons from the cathode to the oxidized dye molecules, thus completing the photo induced charge separation. I^- reduces the sensitizer and is itself oxidized to I^-_3, which gets reduced back to I^- at the cathode. Ordinarily, a platinized TCO glass is used as CE. Platinum (Pt) has established itself as the preferred material for use in CE because of its high catalytic activity and resistance against iodine corrosion.[3] An important research area has been to replace Pt with materials that are cheaper and more abundant. Experiments have shown appreciable performance from carbon-based cathode materials such as mesoporous carbon,[4] hard carbon spherules,[5] activated carbon,[6] carbon black,[7] nanocarbon,[8] carbon nanotubes (CNT),[9,10] conducting polymer,[11] etc. With carbon materials the main problem is that large amounts of it are required to reach close to the efficiency levels of Pt. This makes the device bulkier and completely opaque. CNT CEs have proven to be efficient; however, it is not entirely clear whether this high activity is due to CNTs or is related to the metal oxide particles that are present as impurities along with CNTs.[12,13]

Graphene (G), a novel 2D material with fascinating properties, has become a promising candidate for several electronics and energy based applications like field effect transistors, sensors, Fuel cells etc.[14−16] Earlier in DSSC, G has been implemented a s the transparent conductive anode,[17] as scaffolds for transporting electrons from TiO_2 to the anode[18,19] and even as the sensitizer.[20] G has high conductivity, large surface area, and is easy to produce on an industrial scale at low cost. Recently, Scheuermann et al. reported improved catalytic activity of Pd nanoparticles deposited on G sheets for the Suzuki−Miyaura coupling reaction.[21] Wan et al. have used G films directly as CE in DSSC. However,

Received: June 3, 2011
Accepted: August 30, 2011
Published: August 30, 2011

ACS Publications © 2011 American Chemical Society

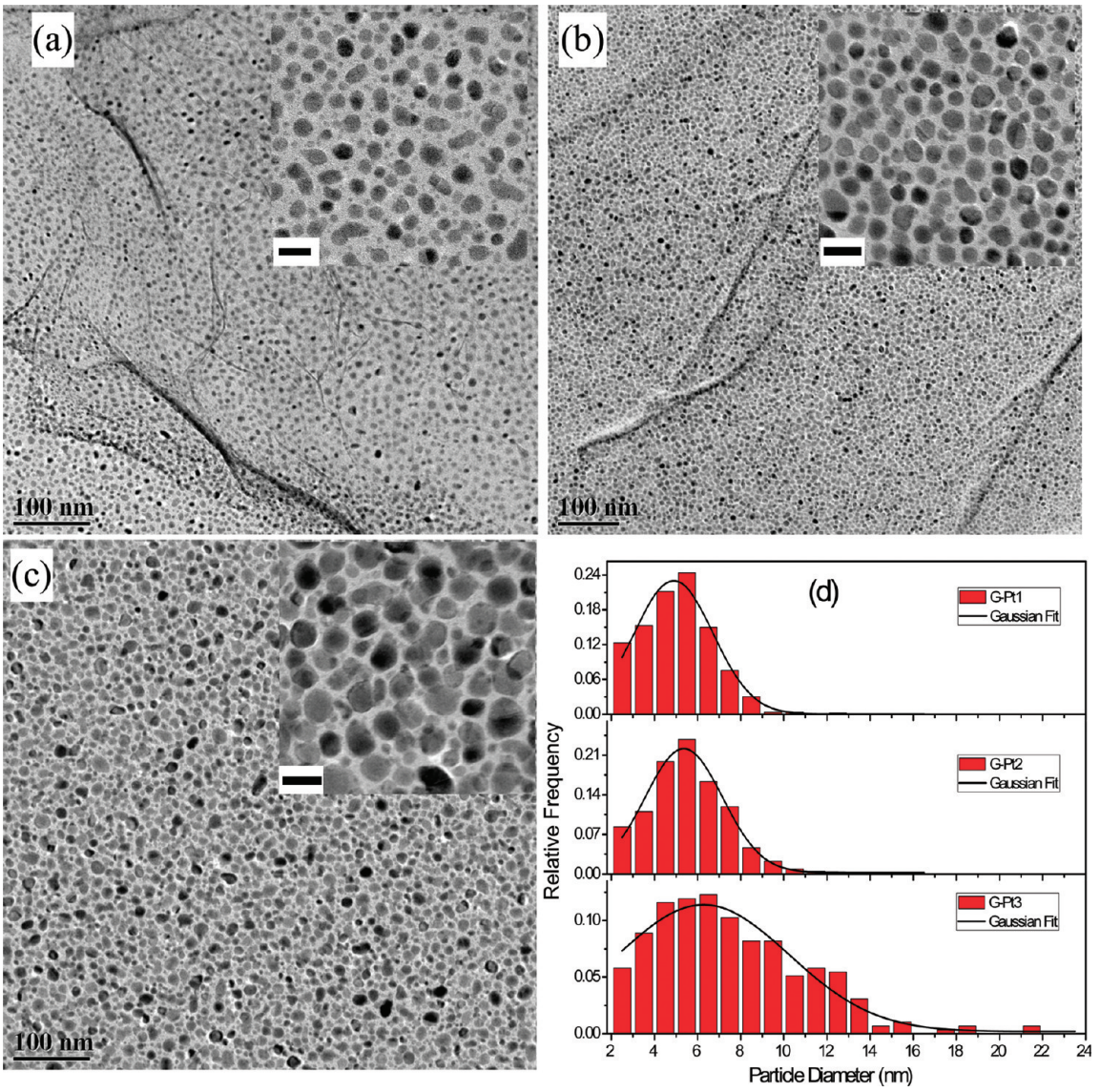

Figure 1. HRTEM images showing composites of G flakes and Pt NP, each having different Pt loadings (a) G-Pt1 (15% Pt), (b) G-Pt2 (27% Pt), and (c) G-Pt3 (34% Pt). Insets show corresponding high-resolution images (scale bars are 10 nm). (d) Particle size distributions along with Gaussian fits.

the efficiency was very low.[22] In our case, too, G films alone were found to be inadequate for proper harnessing of the solar energy. In this report, we are presenting DSSCs that have CEs made from composites of G and Pt nanoparticles (NPs). The G used in these experiments is few layered and produced by one-step thermal exfoliation and reduction of graphite oxide.[23,24] Using pulsed laser deposition (PLD) Pt NPs were deposited uniformly over micrometer-sized G sheets, dispersed on a fluorine doped tin oxide (FTO) coated glass. Such a design of DSSC exhibit better performance than that obtained from Pt thin films or just Pt NP. Superior catalytic property of the composite material for reduction of I_3^- was also established by electrochemical impedance spectroscopy (EIS) and cyclic voltammetry (CV). The main advantage of using G is that one can achieve the same levels of efficiency with much lower amounts of Pt thus opening up the possibility of cost reduction of DSSC. Platinum being scarcely available on earth has to be used economically if DSSCs are to be used to meet large-scale energy demands.

2. RESULTS AND DISCUSSION

The uniform distribution of Pt NPs on G sheets is evident from the high resolution transmission electron microscope (HRTEM) images shown in figure 1. Size distribution of the NPs is depicted in Figure 1d. After 10 s of laser ablation (sample G-Pt1), the particles formed are sparse and discrete having a mean diameter of 5.1 ± 1.7 nm. After 30 s (G-Pt2), the particles become very dense. By now particles start to agglomerate more, resulting in an apparent increase in diameter to 5.5 ± 1.8 nm. G-Pt3 has the longest deposition time, 45 s. A significant number of particles have now fused together forming big clusters and pushing the mean diameter up to 7.6 ± 3.5 nm. The granular surface morphology of a CE formed from the hybrid of G flakes and Pt NPs is shown in a field emission scanning electron microscope (FESEM) image (Figure 2a). The lattice structure of Pt NPs as revealed in a HRTEM is shown in Figure 2b. Composition of the samples was probed via energy dispersive X-ray spectroscopy (EDS). Pt loading in the samples increased as

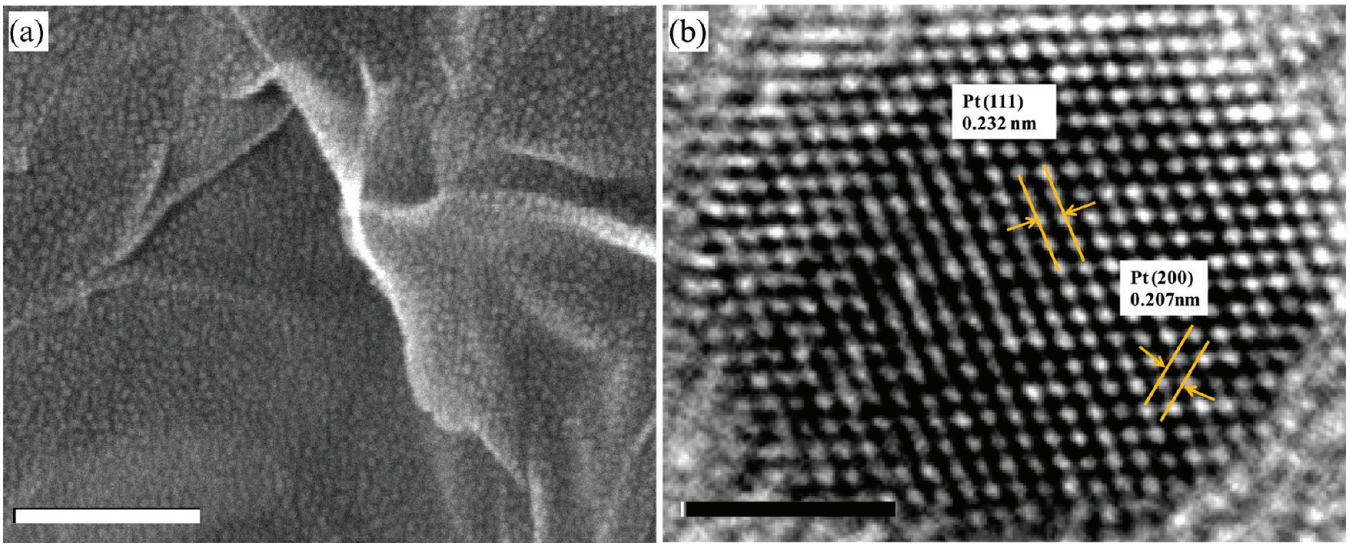

Figure 2. (a) FESEM image of a CE of DSSC showing the dispersed G sheets covered with dense granular looking Pt NPs (scale bar is 100 nm). (b) (111) and (200) lattice planes of a Pt NP as seen inside HRTEM (scale bar is 2 nm).

Table 1. Important Parameters Characterizing Cell Performance and Catalytic Response of the Different CEs along with Their Corresponding Pt Loadings

	G-pt1	G-Pt2	G-Pt3	Pt2	Std-Pt	G
η (%)	2.45	2.91	2.79	2.11	2.00	1.01
J_{sc} (mA.cm^{-2})	5.68	6.67	6.52	5.80	5.05	3.94
V_{oc} (V)	0.73	0.74	0.72	0.69	0.68	0.62
FF	0.59	0.59	0.59	0.53	0.58	0.42
R_{ct} (Ω cm^2)	4.70	2.36	3.04	6.24	7.73	28.23
I_p (mA cm^{-2})	1.27	1.60	1.42	1.20	1.04	0.65
Pt loading (%)	15.17	27.43 [a]	34.27	100 [a]	100 (Pt thin film)	0

[a] These two samples had identical Pt deposition time in PLD.

the deposition time in PLD increased. All results of the current study including the average Pt loading of different samples and the performance parameters of corresponding DSSCs and CEs have been summarized in Table 1.

Current voltage characteristics of the solar cells under 1 sun illumination (AM 1.5, 100 mW/cm^2) are shown in figure 3. Important cell parameters include short circuit current (J_{sc}), open circuit voltage (V_{oc}), power conversion efficiency (η) and fill factor (FF). These are connected by the following equations: $FF = (P_{max})/(J_{sc}V_{oc})$ and $\eta = (P_{max}100)/(P_{in})$,[1,3] where P_{max} is the maximum power output from the cell and P_{in} is the input optical power (100 mW/cm^2). CE containing only G had a reasonable V_{oc} (0.62 V) but poor η (1.01%) and FF (0.42). DSSC assembled with G-Pt2 CE showed the best performance; it had the highest efficiency (2.9%), which is ~45% higher than that of Std Pt-based DSSC (η = 2%). G-Pt2 with higher Pt loading showed better performance than G-Pt1; however, the performance deteriorated slightly (by about 4%) on further increasing the amount of Pt in G-Pt3. We believe this may be due to the formation of larger Pt clusters leading to decreased surface to volume ratio. N. Papageorgiou et al.[25] had made a similar observation while varying Pt loading. They had used thermal decomposition of Pt chloride to make their CEs. S. S. Kim et al.[26] reported that smaller and more uniformly distributed

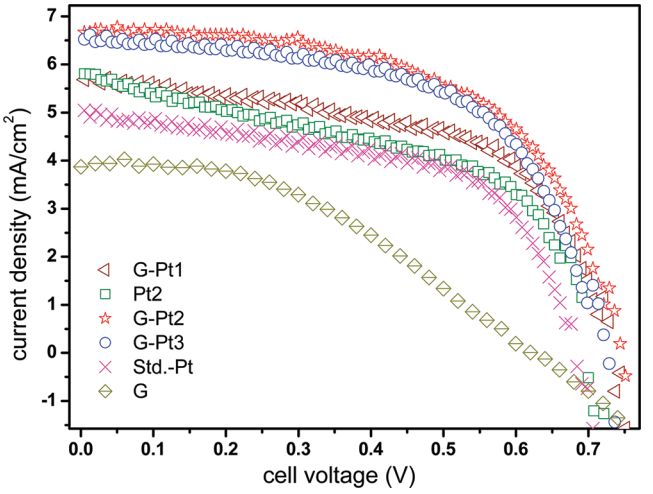

Figure 3. Comparison of $I-V$ characteristics of DSSCs fabricated with different CEs under 1 sun illumination (AM 1.5, 100 mW/cm^2).

Pt NPs have larger specific surface area and perform better as a CE than clustered NPs. Electrodes were prepared by pulse and direct current electrodeposition technique. X. Fang et al.[27] found that there was no significant improvement in efficiency even as the thickness of the Pt film obtained by sputtering was increased from 2 to 415 nm. G-Pt2 composite electrode also showed better performance than its Pt NP counterpart Pt2. Both samples had identical Pt deposition time (30 s) in PLD and hence identical NP content. Inclusion of G sheets in G-Pt2 enabled us to achieve around 38% higher η than Pt2 electrode. There were commensurate improvements in J_{sc} (6.67 mA/cm^2 for G-Pt2), and V_{oc} (0.74 V for G-Pt2) of the composite CEs in comparison with both Pt NP and Std Pt electrodes. However, compared to Std Pt the FF for G-Pt composites showed only marginal improvements (from 0.58 to 0.59), whereas that of Pt NP electrode was lower (0.53). Possible reasons behind the significant performance enhancements of the composite CEs are high catalytic surface area and good conductivity of G. Perfectly crystalline basal plane

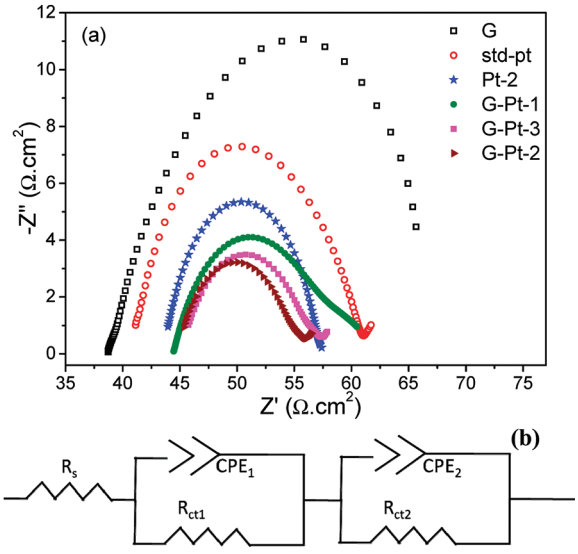

Figure 4. (a) Nyquist plots for the different samples with I^-/I^-_3 redox couple in acetonitrile. Impedances have been normalized wrt the area of the electrodes for easier comparison. (b) Circuit model that was used to fit the EIS spectra.

of graphite is known to have very little catalytic effect.[28] However, the aggressive chemical and thermal techniques employed for production of G introduce significant defect density and oxygen containing functional groups. These provide active sites for I^-_3 reduction to further boost the catalytic activity of Pt. Electrochemically active surface area (ECSA) measurements done previously by others have revealed that G-Pt composites have significantly higher number of catalytically active sites than unsupported Pt NP and commercially available Pt loaded carbon black.[16,29] The advantage of using PLD over other chemical routes to form composites is that it provides a highly ordered coverage and a strong attachment of the NPs on G.[30−32] Proper attachment is instrumental in lowering the interfacial resistance between Pt and G. Recently Huang et al reported DSSC based on composites of CNT with Pt NP. However, the device showed an improvement in η of only 16% over Pt-based DSSC.[10] Hong et al obtained good value of η with composite of G and conducting polymer. But it was lower than that of Pt by about 29%.[33] In this context, the 38−45% increase in efficiency that we report here for the G-Pt composite electrode over the Pt NP and the Pt thin film electrodes is impressive. Additionally, using Pt NP is economically advantageous compared to the more generally used sputtered Pt thin films (20−40 nm).

To investigate the catalytic activity of the electrode materials, we performed EIS and CV measurements. The EIS spectra (nyquist plots) for the different materials are shown in Figure 4a. Variation in the efficiencies of DSSCs fabricated using the different CEs has a one to one correspondence with variation in the charge transfer resistance (R_{ct}) obtained from the nyquist plots (see Table 1). Circuit model used to fit the experimental EIS data is shown in Figure 4b. R_{ct} is a direct measure of the ease of electron exchange between the electrode and the electrolyte. Constant phase element (CPE) is used to model the capacitance which develops at the electrode/electrolyte interface because of the accumulation of ions at the electrode surface. For an inhomogeneous and rough electrode like the ones used in these experiments, CPE is used to simulate the AC response rather

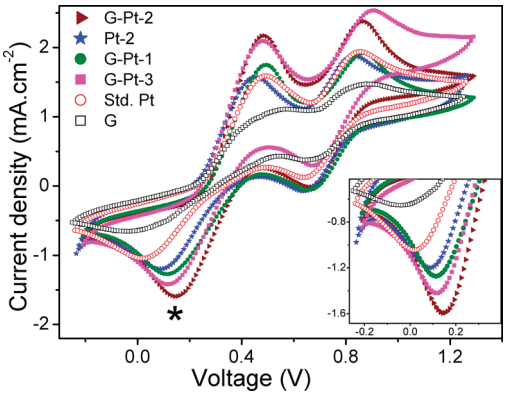

Figure 5. Cyclic voltammograms obtained with the different CEs at a scan rate of 50 mV/s. Reduction peak of I_3^- is marked with '*' and is magnified in the inset.

than an ideal capacitor. The element R_s accounts for the resistance within the bulk of the electrolyte and the electrodes, the contact resistances at the various joints, etc. As can be seen from the nyquist plots, impedance is dominated by the charge transfer process. The effect of diffusion of ions which produces a straight line in the nyquist plot is negligible here. Tiny tails appear in the nyquist plots of some of the electrodes at frequencies close to 1 Hz. These parts have been omitted while modeling, for simplicity. In the modeling circuit used to mimic the EIS set up, the first block consisting of R_{ct1} and CPE_1 represent the auxiliary electrode (a Pt wire) while the second block represent the working electrode (G-Pt1, 2, and 3, Pt2, G, and Std Pt). Similar circuits have been used to model carbonaceous systems earlier.[3] The quantity of interest here is R_{ct}. It varies with Pt loading and drops significantly on addition of G. The lowest value of 2.36 Ω cm^2 was obtained with G-Pt2 samples (Table 1) and it is close to the best reported values in literature.[1,3]

Results of the CV experiments are shown in Figure 5. Two pairs of prominent redox peaks are visible in the CV scan. The second reduction peak marked with '*' is due to the reaction[5,6]

$$I_3^- + 2e^- = 3I^-$$

This is the reaction that takes place at the counter electrode of a DSSC and is vital for its operation. The first peak in CV is due to the reduction of I_2 molecules[5,6] and is unimportant in the context of DSSC. Thus the magnitude of current density at the second reduction peak (I_p) is directly proportional to the ability of the electrode to reduce the I^-_3 species. It is conspicuously larger for the composite electrodes compared to both Pt2 and Std Pt. Variation in I_p follows a pattern similar to both R_{ct} in EIS studies and η of the DSSCs (see Table 1). In addition to this, the reduction peaks and hence the redox potentials of I^-/I_3^- system is shifted slightly toward the positive side in case of the composite electrodes. This could directly lead to higher V_{oc}.[6,34] These results further confirm the superior electrocatalytic activity of G-supported Pt NP electrodes.

3. CONCLUSION

Pt NPs uniformly anchored over G sheets drop casted on FTO were used as CE in DSSC. They outperformed both Pt NP and sputter deposited Pt thin film electrodes. Best efficiencies obtained with G-Pt NP hybrid, Pt NP and Pt thin film were 2.9, 2.11, and 2%, respectively. Thus DSSC fitted with G-Pt composite CE

were ∼45% more efficient than conventional platinized FTO CE and ∼38% more efficient than Pt NP CEs in converting solar energy to electricity. J_{sc} (6.67 mA/cm^2), V_{oc} (0.74 V), and FF (0.59) also improved for the G-Pt composites electrodes. PLD was used to synthesize the composite material. It provided a facile route to controllably achieve highly uniform distribution and strong attachment of NPs on G sheets. The catalytic activity of the Pt NP decorated G sheets when tested with EIS and CV techniques showed lower R_{ct} and higher peak current for I^-_3 reduction, respectively. The lowest R_{ct} obtained with the G-Pt hybrid electrodes was 2.36 Ω cm^2. These results agree well with the observed performance enhancement in DSSC after incorporation of G. The use of G is expected to significantly reduce the cost of DSSC and facilitate mass production by reducing dependence on Pt.

4. EXPERIMENTAL SECTION

G Synthesis. Graphite flakes (average diameter of ∼48 μm) were oxidized in a solution of concentrated sulfuric acid (95−98%), concentrated nitric acid (68%), hydrochloric acid (36−38%), and Potassium chlorate (99.5%) for ∼96 h. Graphite oxide obtained was thermally exfoliated and reduced to produce G platelets. Graphite oxide powder (200 mg) was placed in a quartz tube that was sealed at one end. The other end of the quartz tube was closed using a rubber stopper. An argon inlet was then inserted through the rubber stopper. The sample was flushed with argon for ∼10 min, and the quartz tube was quickly inserted into a tube furnace (Thermolyne 79300, Thermo Fisher Scientific Inc., USA) preheated to ∼1030 °C and held in the furnace for ∼35 s.[23,24]

Counter Electrode of DSSC. One-tenth a milligram of G was dispersed in 50 mL of isopropanol by ultrasonication for ∼12 h. Roughly 500 μL of this solution was drop-casted over FTO-coated glass (TEC 7, Pilkington U.K., with Sheet resistance 8 ohm/□ and thickness 2.2 mm). Pt NPs were deposited onto the G flakes by PLD. The platinum target used in PLD had 99.99% purity. Target and substrate separation within PLD chamber was 42 mm. The third harmonic (355 nm) of Nd:YAG laser, with 10 Hz repetition rate and 5−6 ns pulse width was used to ablate the target. Laser light fluence was kept at ∼2.2 J.cm^{-2}. Deposition was done at a pressure of 4.0×10^{-5} mbar, with a substrate temperature of 450 °C for durations of 10 (G-Pt1), 30 (G-Pt2), and 45 (G-Pt3) seconds. The FTO glass coated with G-Pt composite (G-Pt samples) were used as CEs in the DSSC experiments. G dispersed onto FTO (sample G) and Pt NPs deposited directly on FTO (Pt-2) through PLD, under conditions identical to G-Pt2, were also used as CEs. All results were compared with a thin Pt film (20−25 nm) sputtered onto FTO (Std Pt), which is conventionally used as CE. Sputter deposition was done by using Nordiko2000 sputtering system.

Preparation of Photo Anodes. Titania slurry of total volume 30 cm^3 was made in ethanol with solid loading of 6% v/v. and poly ethylene glycol (PEG) (M_W approximately 600, Thomas baker 99.9%) was used as dispersant as well as binder. Composition of slurry was 7.2 g of TiO_2 (P25 Degussa, average particle size 25 nm, anatase:rutile 75:25) + 7.2 mL of PEG 600 + 21 mL of EtOH. The mixture was milled in a roller mill for 24 h. FTO glass was coated with the TiO_2 paste by doctor blade technique. The TiO_2 films had an area of approximately 4.5 mm × 4.5 mm and thickness of 8−9 μm. The coated film was dried in air and sintered at 450 °C for 1 h. To adsorb the dye molecules, we dipped TiO_2-coated FTO in a dye (Dyesol) made of 0.3 mM N3 (*cis*-bis(isothiocyanato) bis(2,2′-bipyridyl-4,4′-dicarboxylato)-ruthenium(II)) in EtOH and kept undisturbed at room temperature. After 24 h, TiO_2-coated FTO substrates were retrieved from dye solution for use as photo anodes.

DSSC. The DSSC was formed in three steps: (1) A thermoplastic polymer Surlyn of thickness 60 μm was placed across the periphery of TiO_2 film. This works as a sealer as well as a spacer between the photoanode and CE. (2) 2−3 drops of electrolyte were spread over the TiO_2 film. Composition of the electrolyte was 0.6 M PMII (1-methyl-3-propylimidazolium iodide, 98% Aldrich) + 0.5 M LiI (anahydrous, 98%, Merck) + 0.05 I_2 (99.8%, Thomas Baker) + 0.5 M 4-tert butyl pyridine (TBP) (96%, Aldrich) in acetonitrile (Merck). (3) CE was put over the TiO_2 photo anode. And the whole arrangement was clamped.

Characterization. The microstructure and composition of G-Pt NP composite were examined by FESEM (JEOL, JSM-7600F) equipped with EDS spectrometer (Oxford Instrument, INCA Wave) and HRTEM (JEOL, JEM 2100F). To probe the photovoltaic response of DSSC current voltage ($I-V$) characteristics were measured on Keithley 2420 source meter under illumination from Newport class A solar simulator, used to simulate air mass 1.5 G solar radiation of intensity 100 mW cm^2. EIS and CV (Autolab, PGSTAT 302) measurements were done with each CE. EIS spectra were captured in the frequency range of 1 Hz to 1 MHz with 0.01 V applied AC voltage in a two-electrode system. The electrolyte comprised of 0.5 M LiI + 0.05 M I_2 in acetonitrile. CV plots were taken in the voltage range −0.25 to 1.25 V (wrt Ag/AgCl reference electrode in 3 M KCl) at a scan rate of 50 mV/s in a three electrode configuration. The diluted electrolyte for CV consisted of 5 mM LiI + 0.5 mM I_2 + 0.1 M $LiClO_4$ (99.99%, Aldrich) in acetonitrile. A Pt wire was used as counter electrode for both CV and EIS.

AUTHOR INFORMATION

Corresponding Author
*E-mail: drk1955@gmail.com.

Author Contributions
‡Both these authors have contributed equally.

ACKNOWLEDGMENT

Authors acknowledge Prof. Parag Bhargava form Department of Metallurgical Engineering and Materials Science, IIT-B, for allowing unconstrained use of his lab for DSSC measurements. Authors also acknowledge CRNTS and CEN, IIT-B, for facilitating several of the experiments and measurements done in this study.

REFERENCES

(1) Hagfeldt, A.; Boschloo, G.; Sun, L.; Kloo, L.; Pettersson, H. *Chem. Rev.* **2010**, *110*, 6595.
(2) Gratzel, M. *Prog. Photovolt.: Res. Appl.* **2006**, *14*, 429.
(3) Murakami, T. N.; Gratzel, M. *Inorg. Chim. Acta* **2008**, *361*, 572.
(4) Wang, G.; Xing, W.; Zhuo, S. *J. Power Sources* **2009**, *194*, 568.
(5) Huang, Z.; Liu, X.; Li, K.; Li, D.; Luo, Y.; Li, H.; Song, W.; Chen, L.; Meng, Q. *Electrochem. Commun.* **2007**, *9*, 596.
(6) Imoto, K.; Takahashi, K.; Yamaguchi, T.; Komura, T.; Jun-ichi Nakamura, K. Murata *Sol. Energy Mater. Sol .Cells* **2003**, *79*, 459.
(7) Murakami, T. N.; Ito, S.; Wang, Q.; Khaja Nazeeruddin, Md.; Bessho, T.; Cesar, I.; Liska, P.; Robin Humphry-Baker, P.; Comte, P.; Péchy, M. Grätzel *J. Electrochem. Soc.* **2006**, *153*, A2255.
(8) Ramasamy, E.; Lee, W. J.; Lee, D. Y.; Song, J. S. *Appl. Phys. Lett.* **2007**, *90*, 173103.
(9) Lee, W. J.; Ramasamy, E.; Lee, D. Y.; Song, J. S. *ACS Appl. Mater. Interfaces* **2009**, *6*, 1145.
(10) Huang, K. C.; Wang, Y. C.; Dong, R. X.; Tsai, W. C.; Tsai, K. W.; Wang, C. C.; Chen, Y. H.; Vittal, R.; Lin, J. J; Ho, K. C. *J. Mater. Chem.* **2010**, *20*, 4067.
(11) Saito, Y.; Kubo, W.; Kitamura, T.; Wada, Y.; Yanagida, S. *J. Photochem. Photobiol. A: Chem.* **2004**, *164*, 153.
(12) Sÿljukiċ, B.; Banks, C. E.; Compton, R. G. *Nano Lett.* **2006**, *6*, 1556.

(13) Kruusma, J.; Mould, N.; Jurkschat, K.; Crossley, A.; Banks, C. E. *Electrochem. Commun.* **2007**, *9*, 2330.
(14) Kim, B. J.; Jang, H.; Lee, S. K.; Hong, B. H.; Ahn, J. H.; Cho, J. H. *Nano Lett.* **2010**, *10*, 3464.
(15) Robinson, J. T.; Perkins, F. K.; Snow, E. S.; Wei, Z.; Sheehan, P. E. *Nano Lett.* **2008**, *8*, 3137.
(16) Seger, B.; Kamat, P. V. *J. Phys. Chem. C.* **2009**, *113*, 7990.
(17) Wang, X.; Zhi, L.; Mullen, K. *Nano Lett.* **2008**, *8*, 323.
(18) Yang, N.; Zhai, J.; Wang, D.; Chen, Y.; Jiang, L. *ACS Nano* **2010**, *4*, 887.
(19) Tang, Y. B.; Lee, C. S.; Xu, J.; Liu, Z. T.; Chen, Z. H.; He, Z.; Cao, Y. L.; Yuan, G.; Song, H.; Chen, L.; Luo, L.; Cheng, H. M.; Zhang, W. J.; Bello, I.; Lee, S. T. *ACS Nano* **2010**, *4*, 3482.
(20) Yan, X.; Cui, X.; Li, B.; Li, L. S. *Nano Lett.* **2010**, *10*, 1869.
(21) Scheuermann, G. M.; Rumi, L.; Steurer, P.; Bannwarth, W.; Mülhaupt, R. *J. Am. Chem. Soc.* **2009**, *131*, 8262.
(22) Wan, L.; Wang, S.; Wang, X.; Dong, B.; Xu, Z.; Zhang, X.; Yang, B.; Peng, S.; Wang, J.; Xu, C. *Solid State Sci.* **2011**, *13*, 468.
(23) Rafiee, J.; Rafiee, M. A.; Yu, Z. Z.; Koratkar, N. *Adv. Mater.* **2010**, *22*, 2151.
(24) Rafiee, M. A.; Rafiee, J.; Srivastava, I.; Wang, Z.; Song, H.; Yu, Z. Z.; Koratkar, N. *Small* **2010**, *6*, 179.
(25) Papageorgiou, N.; Maier, W. F.; Grätzel, M. *J. Electrochem. Soc.* **1997**, *144*, 876.
(26) Kim, S. S.; Nah, Y. C.; Noh, Y. Y.; Jo, J.; Kim, D. Y. *Electrochim. Acta* **2006**, *51*, 3814.
(27) Fang, X.; Ma, T.; Guan, G.; Akiyama, M.; Kida, T.; Abe, E. *J. Electroanal. Chem.* **2004**, *570*, 257.
(28) Banks, C. E.; Davies, T. J.; Wildgoose, G. G.; Compton, R. G. *Chem. Commun.* **2005**, *18*, 829.
(29) Sharma, S.; Ganguly, A.; Papakonstantinou, P.; Miao, X.; Li, M.; Hutchison, J. L.; Delichatsios, M.; Ukleja, S. *J. Phys. Chem. C.* **2010**, *114*, 19459.
(30) Sohn, J. I.; Nam, C.; Lee, S. *Appl. Surf. Sci.* **2002**, *197*, 568.
(31) Sohn, J. I.; Ok, Y. W.; Seong, T. Y.; Lee, S. *J. Appl. Phys.* **2007**, *102*, 014301.
(32) Diamant, R.; Jimenez, E.; Haro-Poniatowski, E.; Ponce, L.; Fernandez-Guasti, M.; Alonso, J. C. *Diamond Relat. Mater.* **1999**, *8*, 1277.
(33) Hong, W.; Xu, Y.; Lu, G.; Li, C.; Shi, G. *Electrochem. Commun.* **2008**, *10*, 1555.
(34) Dürr, M.; Yasuda, A.; Nelles, G. *Appl. Phys. Lett.* **2006**, *89*, 061110.